LBNL-6062E

ERNEST ORLANDO LAWRENCE
BERKELEY NATIONAL LABORATORY

Quantification of Black Carbon and Other Pollutant Emissions from a Traditional and an Improved Cookstove

Thomas Kirchstetter, Chelsea Preble, Odelle Hadley
and Ashok Gadgil

Environmental Energy Technologies Division
Lawrence Berkeley National Laboratory
Berkeley, CA 94720

November 2010

This work was supported by the Director, Office of Science, Office of Basic Energy Sciences, of the U.S. Department of Energy under Contract No. DE-AC02-05CH11231.

Disclaimer

QUANTIFICATION OF BLACK CARBON AND OTHER POLLUTANT EMISSIONS FROM A TRADITIONAL AND AN IMPROVED COOKSTOVE

Primary Author(s):
Thomas Kirchstetter
Chelsea Preble
Odelle Hadley
Ashok Gadgil

Lawrence Berkeley National Laboratory
One Cyclotron Rd
Berkeley, CA 94720
510-486-5319

Funded by California Energy Commission, Contract Number: 500-99-013

Acknowledgements

The authors gratefully acknowledge Douglas Sullivan and Jessica Granderson of Lawrence Berkeley National Laboratory for their support of this project, as well as the many students, interns, and researchers who, before us, contributed to the development of the Berkeley-Darfur Stove.

ABSTRACT

Traditional methods of cooking in developing regions of the world emit pollutants that endanger the lives of billions of people and contribute to climate change. This study quantifies the emission of pollutants from the Berkeley-Darfur Stove and the traditional three-stone fire at the Lawrence Berkeley National Laboratory cookstove testing facility. The Berkeley-Darfur Stove was designed as a fuel efficient alternative to the three-stone fire to aid refugees in Darfur, who walk long distances from their camps and risk bodily harm in search of wood for cooking. A potential co-benefit of the more fuel efficient stove may be reduced pollutant emissions.

This study measured emissions of carbon dioxide, carbon monoxide, particulate matter, and sunlight-absorbing black carbon. It also measured climate-relevant optical properties of the emitted particulate matter. Pollutant monitors were calibrated specifically for measuring cookstove smoke.

This study found that the Berkeley-Darfur Stove consumed about sixty-five percent of the wood consumed by the three-stone fire and emitted about sixty percent of the carbon monoxide and particulate matter emitted by the three-stone fire when performing the same cooking task. Emissions of black carbon were, on average, lower for the Berkeley-Darfur Stove but this result was not statistically significant due to large test-to-test variability in emissions. Particulate matter emissions of the Berkeley-Darfur Stove were, on the whole, more light absorbing, as evidenced by a reduction in single scattering albedo.

This study supports the notion that wide implementation of efficient cookstoves can reduce the harmful effects of exposure to woodstove smoke and potentially help in mitigating climate change through reduced carbon dioxide emissions. Changes to particulate matter emissions and their sunlight-absorbing properties may also influence climate. Future research should seek to understand why laboratory tests of cookstoves may not accurately reflect their performance in the field so that the health and climate impacts of improved cookstoves can be quantified with greater certainty.

Keywords: improved cookstoves, Berkeley Darfur Stove, three-stone fire, global warming, climate change, indoor air quality, black carbon, particulate matter, carbon monoxide, pollutant emission factor, aethalometer, DustTrak, photoacoustic absorption spectrometer

TABLE OF CONTENTS

EXECUTIVE SUMMARY

Impacts of cookstove air pollution and the Berkeley-Darfur Stove

Exposure to soot and other pollutants emitted from cookstoves in developing regions of the world causes an estimated 1.6 million deaths annually. The burning of wood, dung, agricultural waste, and coal in cookstoves also contributes significantly to the amount of light-absorbing black carbon (BC) emitted to the environment. Studies indicate that BC contributes to global warming and regional climate changes, including altered precipitation and the melting of glaciers. Studies also indicate that BC emitted in Asia may deposit on the Sierra Nevada snowpack, where it may contribute to the observed trend of earlier springtime melting.

This study quantifies the emission of BC and other pollutants from two types of cookstoves: the traditional three-stone fire (TSF) and the Berkeley-Darfur Stove (BDS). The BDS, one of a class of improved cookstoves designed for increased fuel efficiency, was developed to aid Darfur refugee women who face assault when collecting wood for cooking. A potential co-benefit of increased fuel efficiency is reduced emission of air pollutants.

Methodology

This study was performed at the Lawrence Berkeley National Laboratory cookstove testing facility. Cookstove smoke concentrations of BC, fine particulate matter ($PM_{2.5}$), carbon monoxide (CO), carbon dioxide (CO_2) and several climate-relevant particle optical properties were measured. A cookstove smoke-specific calibration was developed for the aethalometer used to measure BC concentrations by comparison with particulate matter light-absorption coefficients measured with a photoacoustic absorption spectrometer and BC concentrations measured using a novel thermal-optical analysis method. The DustTrak used to measure $PM_{2.5}$ concentrations was calibrated against gravimetrically determined concentrations.

The BDS and TSF were compared using a water boiling test intended to simulate the cooking of a common food in Darfur. In this test, a fire was ignited and maintained by periodic addition of wood to raise the temperature of water in a pot to 100 °C and maintain the boil for 15 minutes, whereupon the fire was extinguished and the mass of remaining wood was measured. The mass and moisture content of each piece of wood were measured prior to adding them to the fire.

Emission factors were computed as mass of pollutant emitted per unit mass of wood burned by relating total carbon emissions in the smoke to the carbon content of wood. The mass of pollutants emitted in each test was calculated as the product of test-average pollutant emission factors and the mass of wood burned during each test.

Stove efficiency and pollutant emissions

Approximately 20 tests were conducted with each stove type. The average water heating rate was about 1.6 times larger and the heating rate was more uniform when cooking with the BDS than when cooking with the TSF. On average, tests with the BDS were completed in 73% of the time and with 65% of the wood required for the TSF.

The average CO emission factor (g kg^{-1}) during tests with the BDS was 75% of that for the TSF. The distinction between the stoves is larger when factoring in the higher fuel efficiency of the BDS: on average the BDS emitted 61% of the CO (g) emitted by the TSF for the same cooking

task. The mass of CO emitted in the highest-emitting BDS test was less than the CO emitted in the lowest-emitting TSF test.

Emissions of $PM_{2.5}$ and BC varied more than CO from test to test with both stoves. The average $PM_{2.5}$ emission factor (g kg^{-1}) during tests with the BDS was 80% of that for the TSF. Including the higher fuel efficiency of the BDS, on average the BDS emitted 61% of the $PM_{2.5}$ emitted by the TSF, but as a result of test to test variability, more $PM_{2.5}$ was emitted during some BDS tests than during some TSF tests.

The average BC emission factor (g kg^{-1}) during tests with the BDS was 115% of that for the TSF. In terms of mass emitted, on average the BDS emitted 77% of the BC emitted during tests with the TSF. BC emissions showed a large degree of test to test variability and the distribution of BC emissions with BDS and TSF overlapped considerably.

Since the BDS reduced $PM_{2.5}$ emissions more than BC emissions, relative to the TSF, the emission ratio of $BC/PM_{2.5}$ was larger for the BDS. This compositional difference is reflected in the higher $PM_{2.5}$ mass-specific absorption efficiency (BDS/TSF = 148%), lower single scattering albedo (0.41 for BDS, 0.52 for TSF), and lower absorption Angstrom exponent (1.26 for BDS, 1.51 for TSF) in BDS smoke compared to TSF smoke. The lower single scattering albedo means that the BDS smoke is more sunlight absorbing than the TSF smoke. The lower absorption Angstrom exponent means that on the whole the BDS smoke is blacker than the TSF smoke.

Implications

The current study shows that, in addition to the improved thermal efficiency that leads to increased fuel efficiency, the combustion efficiency of the BDS is higher than that of the TSF. In this study of the BDS, the combined effects of increased fuel and combustion efficiencies reduced by about forty percent CO and $PM_{2.5}$ emissions, respectively, without significantly changing BC emissions when compared to the TSF. Assuming that other similarly designed fuel-efficient stoves share the co-benefit of reduced pollutant emissions, wide implementation of improved stoves could abate the harmful effects of smoke exposure from traditional cookstoves in many developing regions.

The potential to reduce CO_2 emissions by replacing traditional cookstoves with improved cookstoves has prompted the consideration of using improved stoves to abate global-warming. The present study confirms the CO_2 reduction potential of improved stoves: the BDS consumed 65% of the mass of wood consumed by the TSF. It also found differences in particulate matter emissions and optical properties: particulate matter emitted by the BDS absorbed 20% more light (at 532 nm) than particulate matter emitted by the TSF, but the BDS emitted roughly sixty percent of the mass of particulate matter emitted by the TSF. Therefore, improved stoves may impact climate via changes to both particulate matter and CO_2 emissions.

CHAPTER 1: Black Carbon, Environment, and the Berkeley-Darfur Stove

1.1 Black Carbon and Environment

Black carbon (BC) is part of the submicron-sized soot, or fine carbonaceous particulate matter, emitted from most sources of combustion. One type of combustion recently making headlines for its emission of black carbon is cooking in developing countries (Abdollah, 2008; Rosenthal, 2010). Such cooking, which is customarily over an unvented fire of wood, coal, dung, or agricultural waste, contributes significantly to the total amount of BC emitted to the environment (Bond et al., 2004). Exposure to soot and toxic gases, which is highest for women and children, causes an estimated 1.6 million deaths per year (WHO, 2005). Additionally, the inefficient use of solid fuels contributes to deforestation in some regions (Wallmo and Jacobson, 1998). The recent headlines point to another concern: climate change.

BC in the atmosphere absorbs solar radiation and contributes to global warming. A recent study estimated that BC has caused 18% of the planet's warming, compared with 40% for carbon dioxide gas (Ramanathan and Carmichael, 2008). Studies point to important regional effects as well. When BC in the atmosphere absorbs sunlight, less reaches the planet's surface. This causes the atmosphere to warm and surface evaporation of water to decrease, causing decreased precipitation in some regions (Menon et al., 2002). Ultimately, BC deposits on the planet's surface. When deposited on snow and ice, BC darkens the surface and increases the amount of absorbed solar energy (Flanner et al., 2007). By warming the air and reducing snow-albedo, BC may be contributing to the melting of glaciers world-wide (Ramanathan and Carmichael, 2008; Hansen and Nazeranko, 2003). Figure 1 shows the extent to which cooking in developing regions of Asia contribute BC-containing soot that may be accelerating the melting of Himalayan glaciers.

Figure 1: Annual mean optical depth of BC aerosols in 2004-2005 due to BC emission from a) biofuel cooking (with wood, dung, and crop residues), fossil fuels, and biomass burning and b) fossil fuels and biomass burning but not biofuel cooking (Ramanathan and Carmichael, 2008)

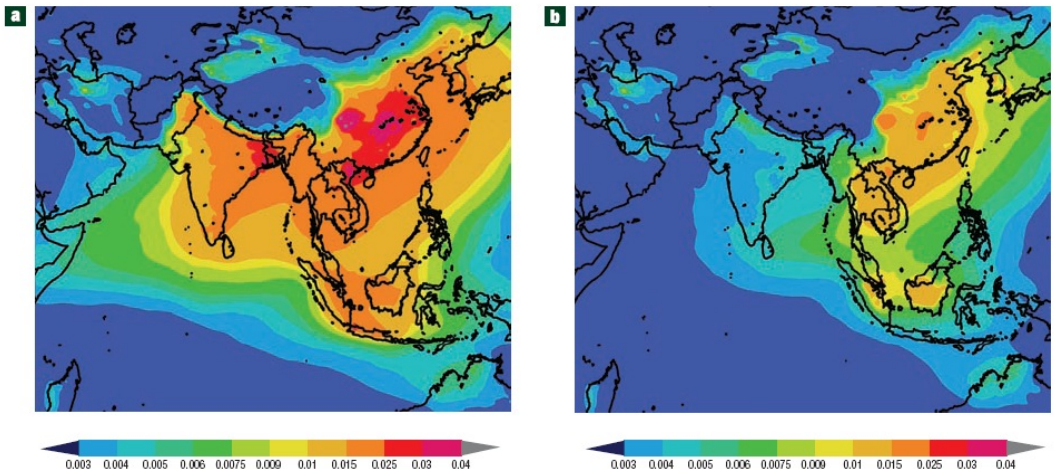

In the Himalayan region, significant ice loss may reduce fresh water availability (Barnett et al., 2005). In regions that critically depend on effective capture and storage of runoff, as in

California where millions of people depend on fresh water reservoirs most of the year, the potential for particulate matter to influence the amount of precipitation in addition to the onset of melt of mountain snowpack is a concern. While it may not be surprising that soot particles emitted from cookstoves in Asia may appreciably darken snow in that region, studies find that particulate matter impacts regions far from the emission source (Huang et al., 2010). One study found that trans-Pacific transport of BC from Asia has the potential to affect coastal mountains in the Western United States (Hadley et al., 2007) especially during springtime when an estimated 25±5% of the BC aerosols deposited on the Sierra Nevada snowpack likely originate from Asia (Hadley et al., 2009).

Stream flow trends indicate earlier onset of melt in California mountain snowpack (Stewart et al., 2004). Compared to 50 years ago, melt begins 10-20 days earlier. The change has been largely attributed to warmer air, but model simulations of the Western United States indicate that BC deposition to snowpack may contribute to early melting (Qian et al., 2009). BC and other particles, emitted locally and transported from Asia, may also be contributing to reduced precipitation in California (Rosenfeld and Givati, 2006). California is presently conducting a multi-year investigation to better understand the impacts of particulate matter on water resources, including suppressed precipitation and enhanced snow melting (NOAA, 2010).

The topic of this report is the emission of BC and other pollutants from cookstoves. With increasing recognition of the health impacts for more than two billion people living in developing regions and the potential climate impacts of cookstoves has come increased efforts to develop improved cookstoves for developing regions (USDOS, 2010). The present study evaluated the traditional three-stone fire (TSF) and a cookstove designed for increased fuel efficiency: the Berkeley-Darfur Stove (BDS).

1.2 The Berkeley-Darfur Stove

The BDS is so named because it was developed by scientists at Lawrence Berkeley National Laboratory and the University of California, Berkeley to aid refugees of the Sudan civil war living in displacement camps in Darfur. Most Darfuri women cook over a "three-stone fire" (TSF). This least expensive class of stove is simply an arrangement of three large stones supporting a pot over an open and unvented fire. In Darfur, women walk up to seven hours, three to five times a week to collect a sufficient amount of wood for cooking. Outside the relative safety of the camps, they are vulnerable to acts of violence and sexual assault. The BDS was designed to use wood more efficiently than the TSF, thereby reducing the amount of time that Darfur refuge women are in harm's way.

A schematic and a picture of the BDS are shown in Figure 2. The schematic points to several design features: 1) a tapered wind collar that increases fuel-efficiency in the windy Darfur environment and allows for multiple pot sizes, 2) wooden handles for easy handling, 3) metal tabs for accommodating flat plates for bread baking, 4) internal ridges for optimal spacing between the stove and a pot for maximum fuel efficiency, 5) feet for stability, 6) nonaligned air openings between the outer stove and inner fire box to accommodate windy conditions, and 7) small fire box opening to prevent using more fuel wood than necessary. The BDS was designed for cultural acceptance by the Darfurians, as it accommodates their traditional round-bottom cooking pot and cooking techniques.

While intended as a more fuel-efficient replacement of the TSF for the people of Darfur, the BDS design elements of increased fuel efficiency are intrinsic to stoves designed for implementation in other developing regions of the world. Moreover, the BDS and similar stoves may have the co-benefit of reduced pollutant emissions. Nearly half of the world's population cooks a portion

of their food over open fire, so widespread use of improved-efficiency cookstoves like the BDS could have tremendously beneficial impacts on health and the environment.

Figure 2: Schematic and picture of the Berkeley-Darfur Stove. The schematic illustrates several design features that are described in the text above.

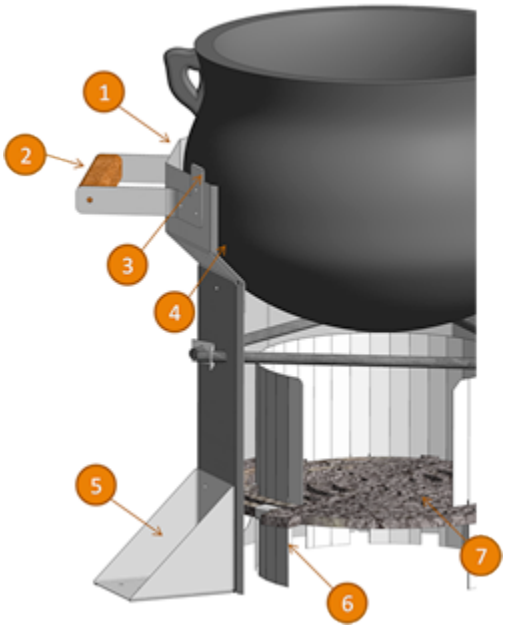

Photo Credit: Lawrence Berkeley National Laboratory

1.3 Project Objectives

The goal of this research is to measure and compare the emission of pollutants from the BDS and TSF. The focus is on sunlight-absorbing BC but includes fine particulate matter ($PM_{2.5}$), carbon monoxide (CO), carbon dioxide (CO_2) and several climate-relevant particle optical properties as well. It is anticipated that the information generated in this and in similar studies will aid in evaluating potential health and climate benefits of replacing traditional cookstoves with improved cookstoves. Considerable effort is devoted in this study to developing woodsmoke specific calibrations of analyzers used to measure time-resolved BC and $PM_{2.5}$ concentrations to ensure accuracy and to demonstrate their general suitability for characterizing cookstove emissions.

CHAPTER 2: Cookstove Testing Methodology

2.1 Cookstove Testing Facility

This study was performed at the Lawrence Berkeley National Laboratory. A schematic of the cookstove testing facility is shown in Figure 3. Cooking was carried out on a platform underneath a plenum. A blower connected to the plenum via an aluminum duct (15 cm in diameter) drew the smoke from cooking fires and room air into the plenum. The smoke and room air mixed along the length of the duct, aided by stationary fan blades, turns in the duct, and turbulent flow. At a point prior to the blower, diluted smoke was drawn via stainless steel tubing (1.1 cm in diameter) through a very sharp cut cyclone (BGI, model VSCCA) to remove particles with diameters larger than 2.5 μm. Downstream of the cyclone, the sample flow was split using two-way stainless steel flow splitters (BMI, models 1100 – 1102) and sampled with several instruments listed in Table 1. Dry, particle-free air was mixed with a portion of the flow to further dilute the particulate matter concentration by about a factor of 10 prior to sampling, as illustrated in Figure 3.

Figure 3: Schematic of the cookstove testing facility at Lawrence Berkeley National Laboratory.

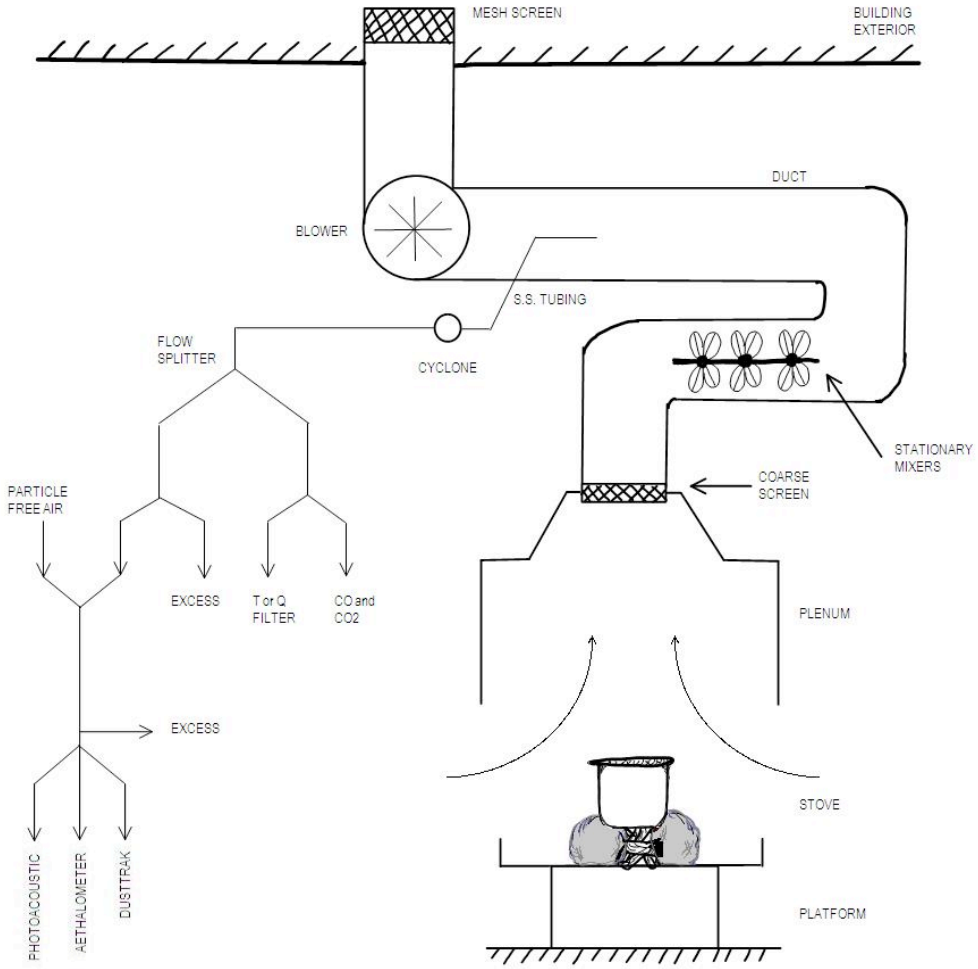

Table 1: Instrumentation used to quantify pollutant emissions

	Parameter	Instrument	Primary or Secondary Products
Time-Resolved (1 Hz)	CO and CO_2 concentrations	NDIR analyzer (CAI 600 series)	Combustion efficiency; fuel-based pollutant emission factors (g kg^{-1})
	$PM_{2.5}$ concentration	DustTrak (TSI 8534)	BC and $PM_{2.5}$ fuel-based emission factors (g kg^{-1}); particle mass absorption efficiency (m^2 g^{-1}); particle single scattering albedo
	BC concentration	Aethalometer (Magee Scientific AE16)	
	Absorption and scattering coefficients	Photoacoustic absorption, reciprocal nephelometry (custom)	
	Absorption coefficient at 3-wavelengths	Particle-soot absorption photometer (Radiance Research)	Absorption spectral selectivity (particle color)
	Duct and food temperature	Thermocouples	Food heating rate; test duration
	Duct pressure	Pressure sensor	Dilution flow rate
Time-Integrated	$PM_{2.5}$ mass	Teflon filter; gravimetric analysis	Calibration of DustTrak
	BC mass	Quartz filter; thermal-optical analysis	Calibration of Aethalometer
	Wood mass	Balance & moisture meter	Dry wood addition rate

The concentrations of CO, CO_2, BC, and $PM_{2.5}$, particle absorption and scattering coefficients, duct pressure, and temperature are measured at 1 Hz. CO and CO_2 concentrations were measured in a single instrument by nondispersive infrared absorption spectroscopy. $PM_{2.5}$ and BC concentrations were measured using a DustTrak and aethalometer, respectively. Absorption and scattering coefficients at a wavelength of 532 nm were measured using a custom-made instrument employing photoacoustic absorption (Arnott et al., 1999) and reciprocal nephelometry (Penaloza, 1999). For simplicity, we refer to this instrument as a photoacoustic absorption spectrometer (PAS). A three-wavelength particle soot-absorption photometer (PSAP) that monitors light-absorption at 467, 530, and 660 nm (Virkkula et al., 2005) was used to

measure the light-absorption wavelength-selectivity of particulate matter. Each of these particulate-phase measurements are further discussed below.

Time-integrated measurements of BC and $PM_{2.5}$ concentrations based on the analysis of filters periodically collected during cooking tests were used to develop calibration equations specific to woodsmoke for the aethalometer and DustTrak. The mass of $PM_{2.5}$ collected on Teflon filters was measured using a microbalance. The mass of BC collected on quartz fiber filters was measured by the thermal-optical analysis (TOA) method described by Hadley et al. (2008).

The flow rates of each sample line and the secondary particle dilution rate illustrated in Figure 3 were measured daily with a primary standard air flow calibrator (Sensidyne, Gilibrator-2). The measured flows were used to calculate filter-based BC and $PM_{2.5}$ concentrations and scale upwards the optical coefficients, BC concentrations, and $PM_{2.5}$ concentrations measured with the photoacoustic absorption spectrometer, aethalometer, and DustTrak, respectively, that were subject to secondary dilution.

A calibrated air flow measurement system (The Energy Conservatory, Duct Blaster System) was used to establish the relationship between the flow rate of air into the exhaust plenum and the pressure and temperature at a fixed point inside the exhaust duct. The flow rate of air into the exhaust system during stove tests was estimated from this calibration relationship and the duct pressure and temperature, which were measured at 1 Hz.

2.2 Instrument Operating Principles and Calibration

2.2.1 Aethalometer and TOA BC

The aethalometer continuously filters air and measures the amount of light attenuated (ATN) by collected particles: $ATN = -100(I/I_o)$, where I and I_o are the final and initial intensities of light transmitted through the filter over a period of time. The filter darkens until the value of ATN reaches a preset threshold and the filter is advanced, after which the next sampling cycle begins with a fresh filter. ATN is assumed to be proportional to the mass of BC: BC ($\mu g\ cm^2$) = ATN/□, where ATN is measured at a wavelength of 880 nm and □ is a calibration constant equal to 16.6 $m^2\ g^{-1}$ that the aethalometer uses to convert particle light absorption to BC mass concentration. It is generally acknowledged that BC is the only particulate matter with appreciable absorption at 880 nm.

A known sampling artifact causes a diminishing response to BC as the aethalometer's filter darkens. Kirchstetter and Novakov (2007) developed an equation to correct aethalometer BC data for this sampling artifact:

$$BC_{corrected} = \frac{BC_0}{0.88\exp\left(\frac{-ATN}{100}\right) + 0.12} \quad (1)$$

The applicability of this equation to cookstove emissions is verified in this study by comparing aethalometer BC measurements to absorption coefficients measured simultaneously with the photoacoustic absorption spectrometer. Both of these instruments respond to light absorbing particulate matter, so their responses are nominally proportional in the absence of sampling artifacts. (The photoacoustic absorption spectrometer operates at 532 nm where, in addition to BC, organic compounds in woodsmoke absorb light; else the response of these two instruments

should be exactly proportional.) Data for one cooking test are shown in Figure 4, where the ratio of absorption coefficient to BC concentration is plotted as a function of the ATN level of the aethalometer's filter. Using unadjusted BC data (BC_o), this ratio continuously increased from 10 to greater than 25 $m^2\ g^{-1}$ as the aethalometer's filter increasingly loaded. Using BC data corrected with equation 1 ($BC_{corrected}$), the ratio is approximately constant. The data from other cooking tests are consistent with those shown in Figure 4. Since there is no physical basis for continually increasing BC and the ratio of absorption coefficient to BC concentration is expected to be approximately constant, this comparison verifies that equation 1 is applicable in this study. Moreover, this comparison illustrates the magnitude of the potential error as corrected BC concentrations are 250% larger than unadjusted BC concentrations at the end of the aethalometer's sampling cycle.

Two additional terms are used in this study to further adjust aethalometer data, as written in equation 2. The term *flow* (equal to 1.28) is included because the sampling flow rate measured by the aethalometer (1.0 L min^{-1}) differed from the flow rate measured with the air flow calibrator (1.28 L min^{-1}). The term *cal* (equal to 1.15) is based on a comparison of BC concentrations of the aethalometer (after applying equation 1 and adjusting for secondary dilution) and those measured by TOA, shown in Figure 5.

In TOA, the carbon contained in particulate matter is evolved through heating while the transmission of light through the sample is monitored. The optical characterization aids in the discrimination between organic carbon and BC and in traditional TOA methods is monochromatic. The TOA method used in this study is a recent advance over traditional methods that measures the spectral variation in light transmitted through the sample and refines estimates of BC based on the different spectral absorption selectivities of BC and other light-absorbing organic compounds, as described by Hadley et al. (2008).

$$BC_{corrected} = \left[\frac{BC_0}{0.88\exp\left(\frac{-ATN}{100}\right)+0.12}\right]\left[\frac{cal}{flow}\right] \quad (2)$$

Figure 4: Evidence of need to correct aethalometer data and verification of correction equation 1

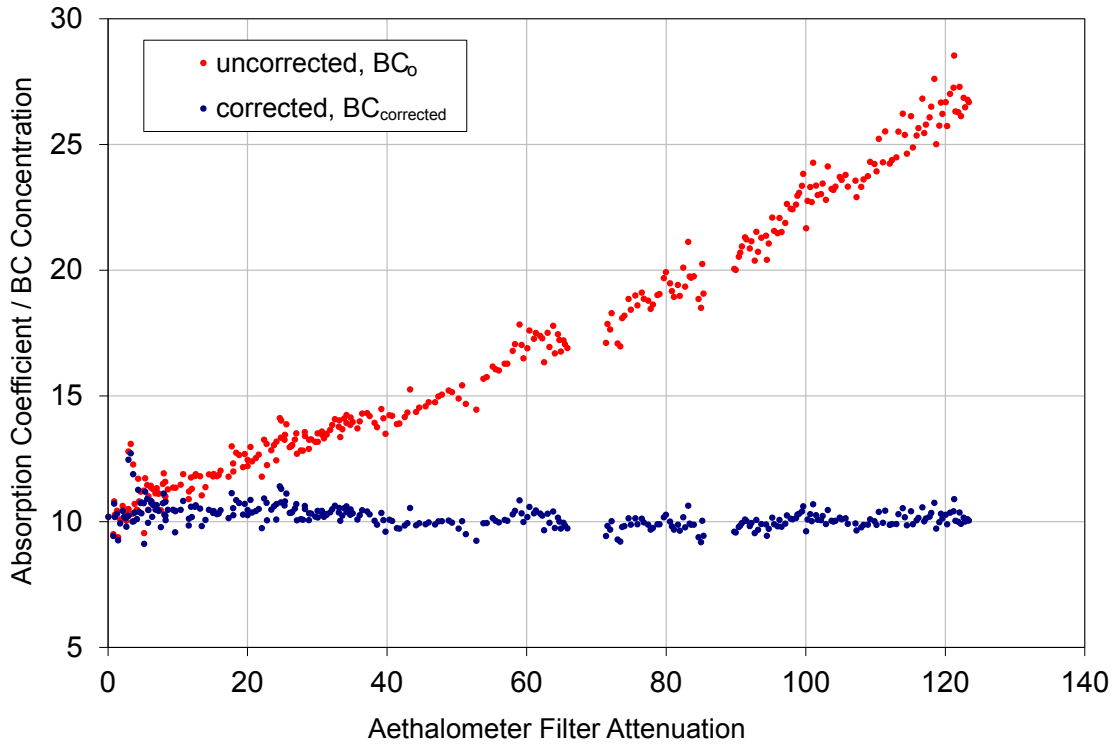

Figure 5: Relationship between BC concentrations measured with the aethalometer and by thermal-optical analysis of quartz filters

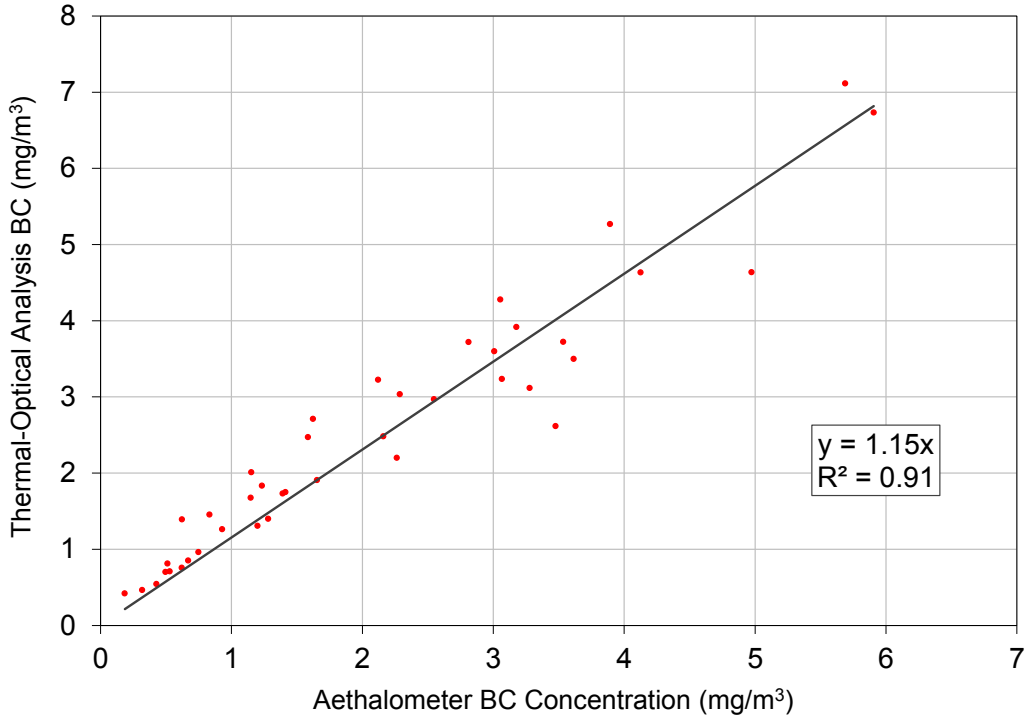

2.2.2 DustTrak and Gravimetric $PM_{2.5}$

The DustTrak measures the amount of light scattered by particles and relates that to their mass. It is calibrated for a NIST certified PM standard composed of soil from Arizona. Since the amount of light scattered by particles is specific to their morphology and chemical composition, in this study a calibration specific to woodsmoke was developed, per the manufacturer's recommendation, by comparing $PM_{2.5}$ concentrations measured with the DustTrak after adjusting for secondary dilution (PM_o) to those measured gravimetrically:

$$PM_{corrected} = 1.10(PM_0)^{0.78} \quad (3)$$

The mass of particles collected on Teflon filters was measured using a microbalance after conditioning overnight at 40% RH (i.e., drying) to be consistent with the air sampled by the DustTrak, which was dried as a result of dilution with dry air as shown in Figure 3.

Figure 6: Relationship between $PM_{2.5}$ concentrations measured with the DustTrak and by gravimetric analysis of Teflon filters

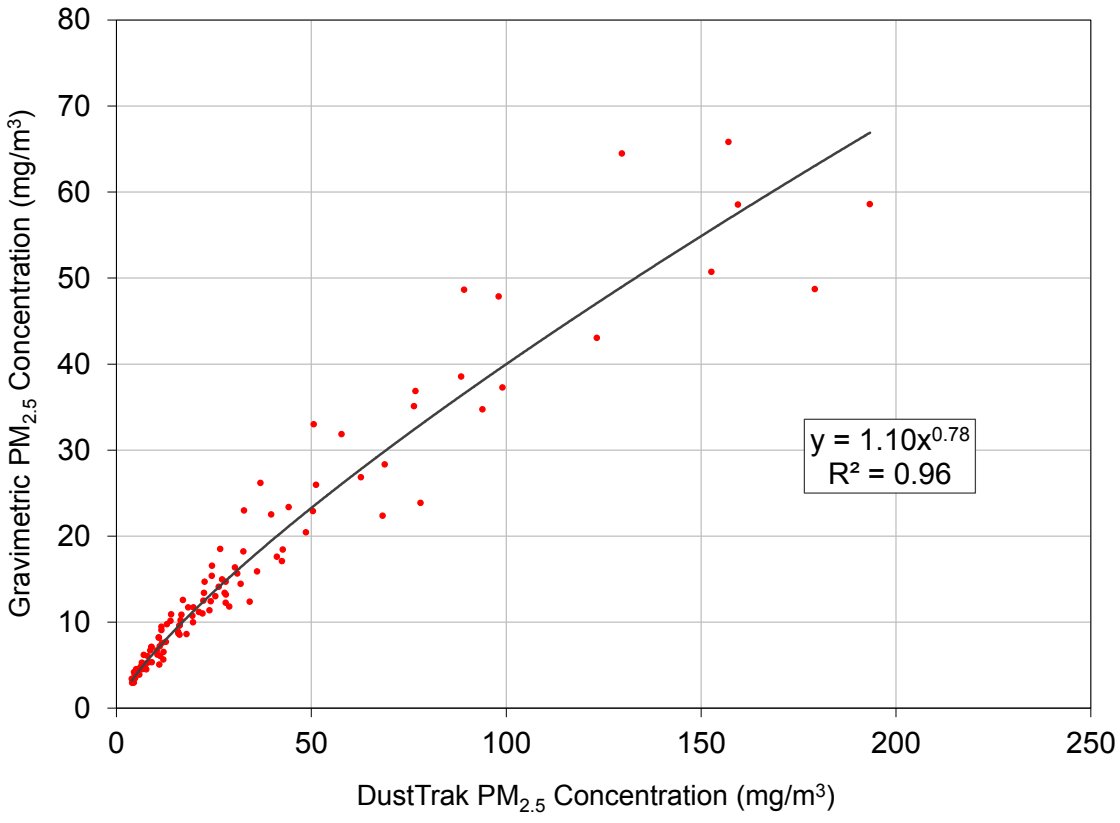

2.2.3 PAS and PSAP Particle Optical Properties

The photoacoustic absorption spectrometer measures the sound produced when particles heated with a 532 nm laser in an acoustic resonator transfer heat to the surrounding air. From this measurement and the laser power, aerosol light absorption (b_{abs}) is calculated (Arnott et al., 1999). The instrument simultaneously measures scattering coefficient (b_{scat}) at the same wavelength in a separate cell employing the principle of reciprocal nephelometry (Penaloza, 1999). Airflow into the instrument is split between the photoacoustic and nephelometer cells and flows into these cells are set so that the time constant of each cell is similar. The calibration of this instrument was verified as described by Arnott et al. (2000), using ammonium sulfate and soot particulate matter prior to this study.

As a result of sample dilution (as noted above and shown in Figure 3), the relative humidity measured inside the photoacoustic instrument was typically 10%. This is sufficiently dry to result in efflorescence, so the sampled particulate matter is presumed to be dry. Thus, the photoacoustic measurement was not likely affected by the evaporation of water from particle surfaces and the scattering of light by particles was not enhanced by water-increased particle cross-section.

The single scattering albedo (SSA), the climate-relevant parameter that is equal to the fraction of incident light scattered as opposed to absorbed, is calculated from the measured particle optical coefficients:

$$SSA(532nm) = \frac{b_{scat}}{(b_{scat} + b_{abs})} \tag{4}$$

where the sum in the denominator is equal to total extinction. Absorption and scattering coefficients are divided by $PM_{2.5}$ concentration to calculate mass-specific absorption (MAE) and scattering (MSE) efficiencies (in units of $m^2\ g^{-1}$), respectively

$$MAE(532nm) = \frac{b_{abs}}{PM_{2.5}} \tag{5}$$

$$MSE(532nm) = \frac{b_{scat}}{PM_{2.5}} \tag{6}$$

The PSAP continuously measures the transmission of light through a white fibrous filter as it darkens with particles. Unlike the PAS that measures light-absorption of particulate matter suspended in air, the PSAP measurement of light-absorption is subject to errors associated with the embedment of particulate matter in a highly reflective filter (Cappa et al., 2008; Virkkula et al., 2005; Bond et al., 1999). Therefore, rather than use the PSAP to measure absorption coefficients absolutely, it is used in this study to estimate the absorption Angstrom exponent (AAE), which is a measure of the variation in light-absorption with wavelength.

The AAE, like the SSA, is a climate- relevant property of particulate matter and is especially relevant to woodsmoke. Absorption selectivity is relatively weak for BC and strong for light-

absorbing organic particulate matter in wood smoke, which is therefore not black but a shade of brown (Andreae and Gelenscer, 2006). Fitting the trend in absorption coefficients versus wavelength (□) with a power law equation yields the AAE:

$$b_{abs}(\square) = \text{constant} \times \square^{-AAE} \quad (7)$$

which is approximately 1 when BC is the primary light absorber and larger than 1 when brown carbon is present, as it is in woodsmoke (Kirchstetter et al, 2004).

2.2.4 Cooking Tests

The BDS and TSF are compared in this study using the same cooking test, which featured the boiling of water. Like other water boiling tests intended to mimic cooking food, this test is intended to simulate the cooking of Assida, a common food in Darfur (Galitsky et al., 2005). In this test, a wood fire was ignited by burning one sheet of crumpled newspaper, and 2.5 L of water in a 2.3 kg metal Darfur pot was heated from an average temperature of 21±4 °C (±1 standard deviation) to 100°C. The temperature of the water was recorded using a digital thermometer equipped with a type K thermocouple. After the water began to boil, a flaming fire was maintained and the water temperature was not permitted to drop below 94 °C for 15 minutes. After this 15 minute period, the fire was extinguished so that the remaining mass of wood could be measured. This test, therefore, does not capture pollutant emissions under exclusively smoldering conditions that occur when flames extinguish.

The mass of wood used during ignition, throughout the test, and remaining at the end 15 minute boil period was measured using an analytical balance. The accuracy of the balance up to 100 g was verified using a set of standard weights. After igniting slivers of wood, fires were maintained with approximately 7 pieces of wood in the stove to bring the water to boil (high-power phase) and approximately 4 pieces of wood in the stove during the subsequent 15 minute period (low-power phase). The tester arranged wood pieces to maintain the fire and occasionally used a bellows to blow on the fire when it prematurely extinguished. These actions and the rate of addition of wood were recorded in a laboratory notebook during tests.

The moisture content of each piece of wood was measured using a moisture meter (Delmhorst, J-2000). The equivalent dry mass of each piece of wood (m_{dry}) was calculated as:

$$m_{dry} = \frac{m_{wet}}{\left(1 + f_m\right)} \quad (8)$$

where m_{wet} is the mass of wood measured with the scale and f_m is the measured wood moisture content.

Soft (pine and fir) and hard (oak) woods were used in an equal number of tests with both stove types. Soft wood pieces were saw-cut to approximately 15 cm long with a square cross-section of approximately 4 cm^2 and hard wood pieces were hatchet-cut to a similar size but irregular shape. The moisture content and dry mass of the soft and hard woods were similar to each other and were the same for TSF and BDS tests. The moisture content of soft wood (9±2 %) and

hard wood (10±2 %) pieces was essentially the same. The dry mass of soft (20±9 g) and hard wood (26± 13 g) pieces was similar.

2.2.4 Pollutant Emission Calculations

Emission factors were computed as mass of pollutant emitted per unit mass of wood burned by relating total carbon emissions in the fire (mainly in the form of CO and CO_2) to the carbon content of wood using the following equation:

$$EF_P = 10^3 \left[\frac{\Delta[P]}{\Delta[CO] + \Delta[CO_2]} \right] w_c \quad (9)$$

where EF_P is the emission factor (g emitted per kg of fuel burned) for pollutant P, Δ[P] is the increase in the concentration of pollutant P (μg m^{-3}) above background levels, Δ[CO] and Δ[CO_2] are the increases in the concentrations of CO and CO_2 (μg of carbon m^{-3}) above background levels, and w_c is the fraction of carbon in wood. The carbon weight fraction of wood was assumed in this study to be 0.5 (g carbon per gram of wood) based on literature values (Gaur and Reed, 1998). Background levels of all species except CO_2 were negligible compared to concentrations measured in the woodsmoke in this study. Background CO_2 concentrations were measured prior to the ignition of each fire.

Fuel-based emission factors were computed for each cooking test using test-average pollutant concentrations. The total mass (g) of a pollutant emitted in each test was calculated as the product of the test-average fuel-based emission factor and the measured mass of wood burned during the test.

Highly time-resolved pollutant emission factors were computed based on the estimated system flow rate:

$$IEF_P = \Delta[P] \times Q \quad (10)$$

where IEF_P is the "instantaneous" emission factor (μg emitted per s) for pollutant P, Δ[P] is the same as defined above, and Q is the flow rate of air (m^3 s^{-1}) into the exhaust plenum.

CHAPTER 3: Stove Efficiency and Pollutant Emissions

The data presented below are the result of 21 tests with the BDS and 20 tests with the TSF. An equal number of prior tests were conducted to optimize and develop consistency in sampling, measurement, and cooking methods. In general, all instrumentation discussed above and shown in Figure 3 properly operated during these 41 tests with one notable exception – the PSAP was unavailable at the time of these 41 tests. The AAE values derived from the PSAP data are the result of 15 separate tests.

3.1 Stove Efficiency

Figure 7 shows the water temperature measured during 40 tests. The average heating rate was about 1.6 times larger and the heating rate was more uniform when cooking with the BDS than when cooking with the TSF. The distribution of test durations and wood consumption is shown in Figures 8 and 9, respectively. On average, tests with the BDS were completed in 73% of the time and with 65% of the wood required for the TSF. In both cases, there was less variation with the BDS, as indicated by the narrower distributions and the smaller standard deviations.

On average, tests with soft wood were completed in about 90% of the time and with 90% of the wood compared to tests with hard wood. The relative efficiency of the BDS and the TSF – measured in time and dry wood consumed – was essentially the same for both wood types.

Figure 7: Water temperature during BDS (solid red lines) and TSF (solid black lines) cooking tests, representative heating rates (dashed lines), and ranges of time required to boil (shaded regions)

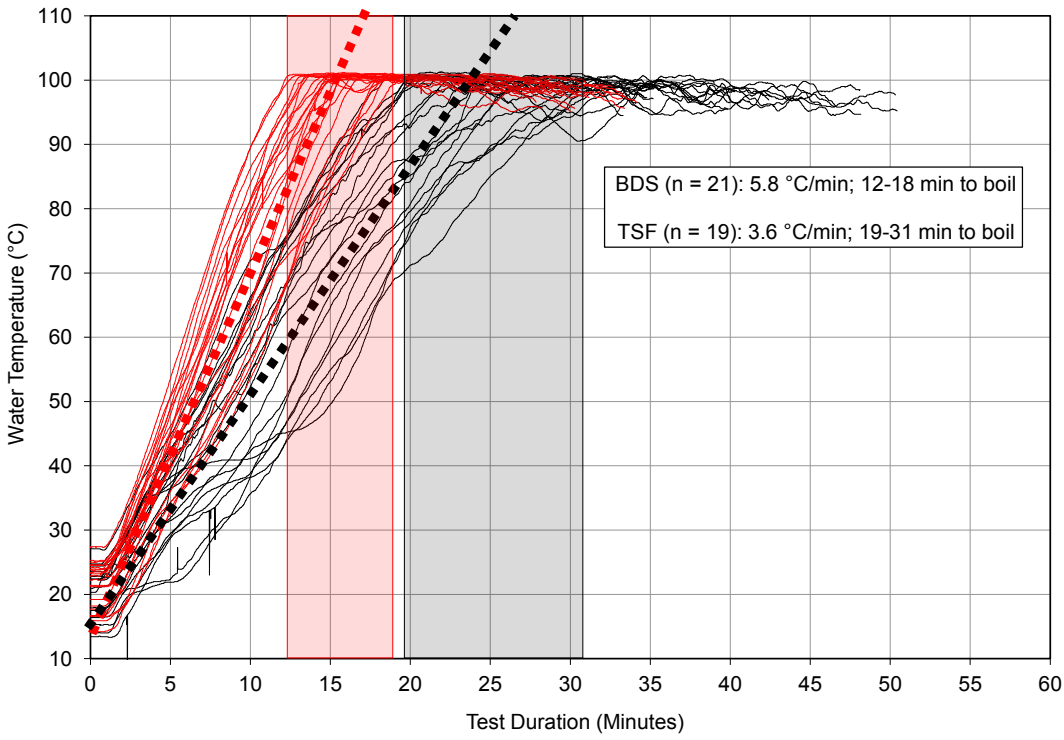

Figure 8: Distribution of test durations when cooking with the BDS and TSF

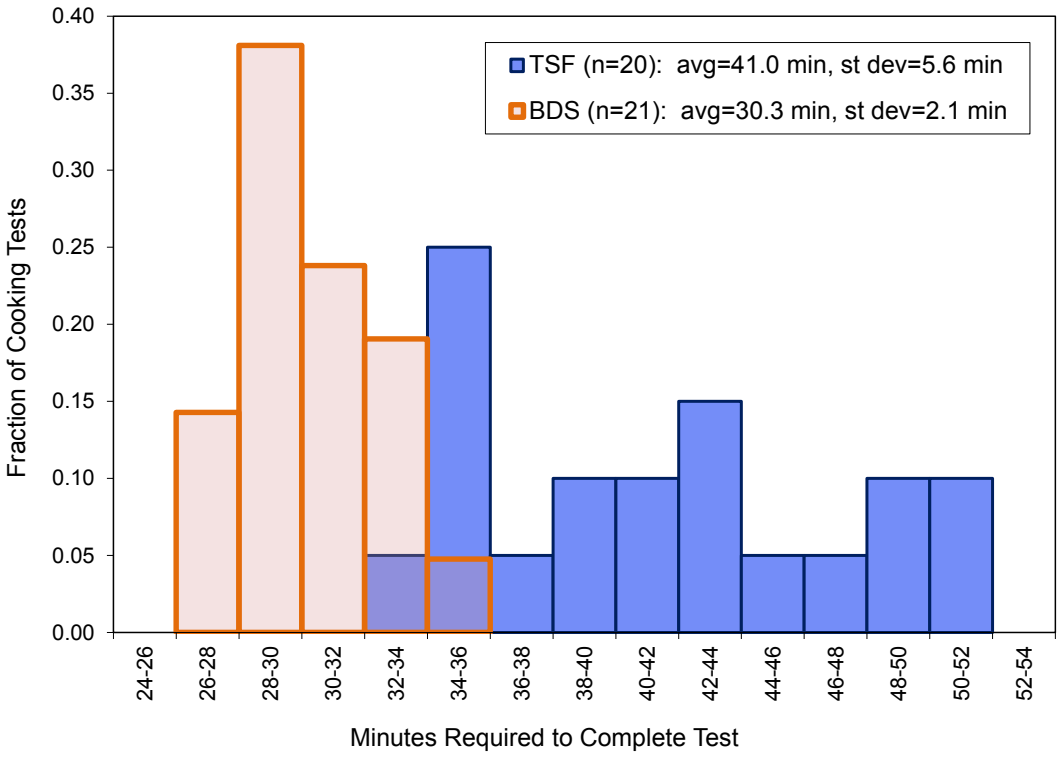

Figure 9: Distribution of dry wood consumption when cooking with the BDS and TSF

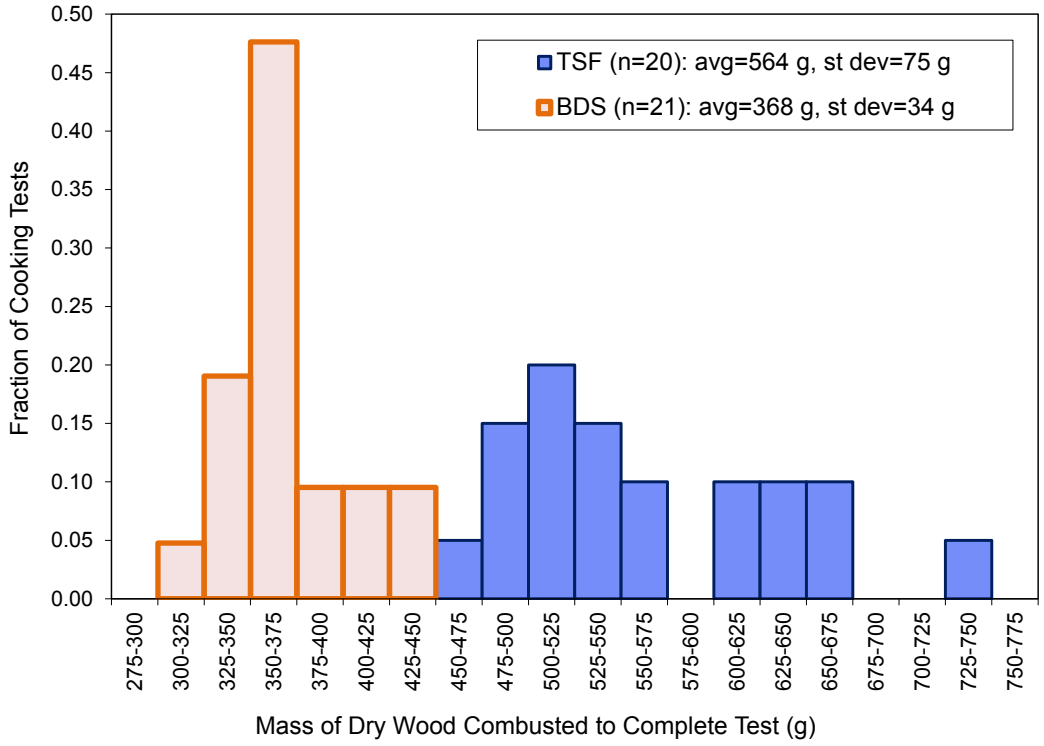

3.2 Pollutant Emissions

Pollutant emission factors were computed with equation 9 for each test from the pollutant concentrations shown in table A1 and A2. Results are tabulated in table A3 and A4 and summarized in Figures 10, 11, and 12, which show for CO, $PM_{2.5}$, and BC, respectively, the distribution of fuel-based emission factors (g kg^{-1}) and the distribution of mass emissions (g) measured in tests with the BDS and TSF.

Of these three pollutants, the clearest distinction between the BDS and TSF is observed for CO, as evidenced by the separation in the distributions shown in Figure 10 compared to Figures 11 and 12. The average CO emission factor (g kg^{-1}) during tests with the BDS was 75% of that for the TSF. The distinction between the stoves is larger when factoring in the higher fuel efficiency of the BDS: on average the BDS emitted 61% of the CO (g) emitted by the TSF for the same cooking task. The mass of CO emitted in the highest-emitting BDS test was less than the CO emitted in the lowest-emitting TSF test, as evidenced by the complete separation of the emission distributions.

Emissions of $PM_{2.5}$ and BC varied more than CO from test to test with both stoves. The average $PM_{2.5}$ emission factor (g kg^{-1}) during tests with the BDS was 80% of that for the TSF. Including the higher fuel efficiency of the BDS, on average the BDS emitted 61% of the $PM_{2.5}$ emitted by the TSF, but as a result of test to test variability, more $PM_{2.5}$ was emitted during some BDS tests than during some TSF tests.

Figure 10: Distribution of CO fuel-based emission factor (left) and mass of CO emitted (right) in cooking tests with the BDS and TSF

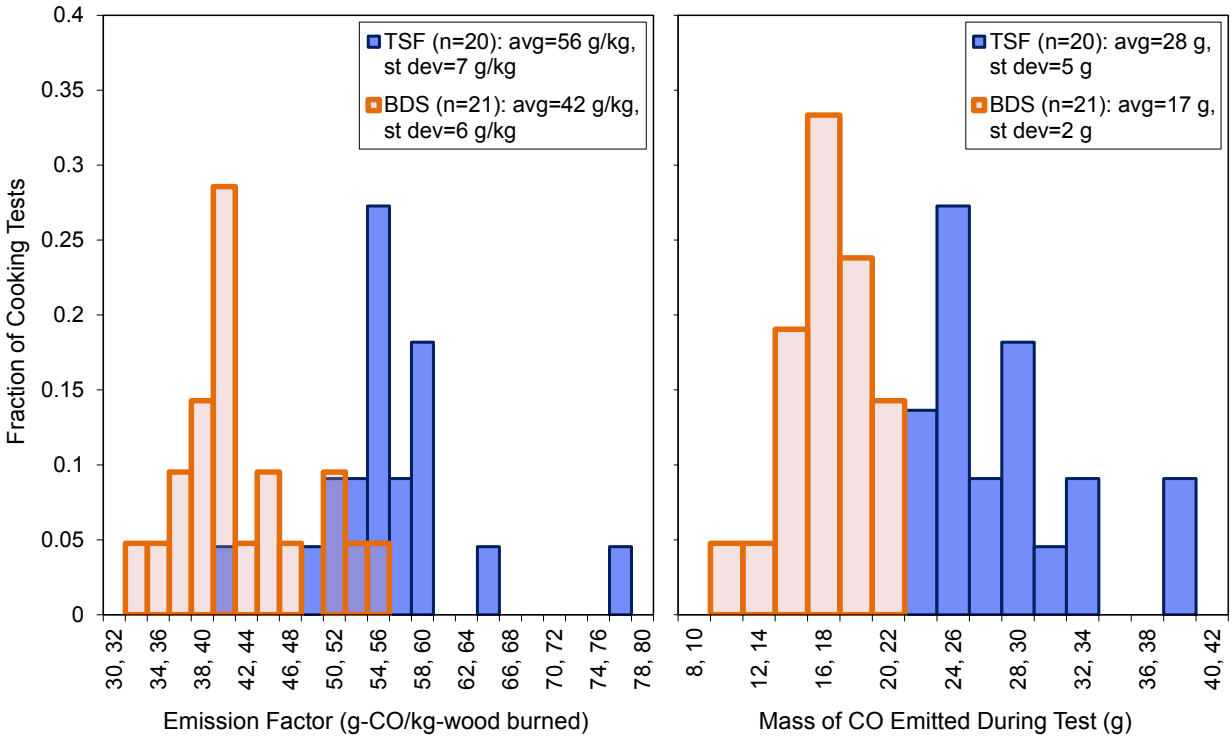

Figure 11: Distribution of $PM_{2.5}$ fuel-based emission factor (left) and mass of $PM_{2.5}$ emitted (right) in cooking tests with the BDS and TSF

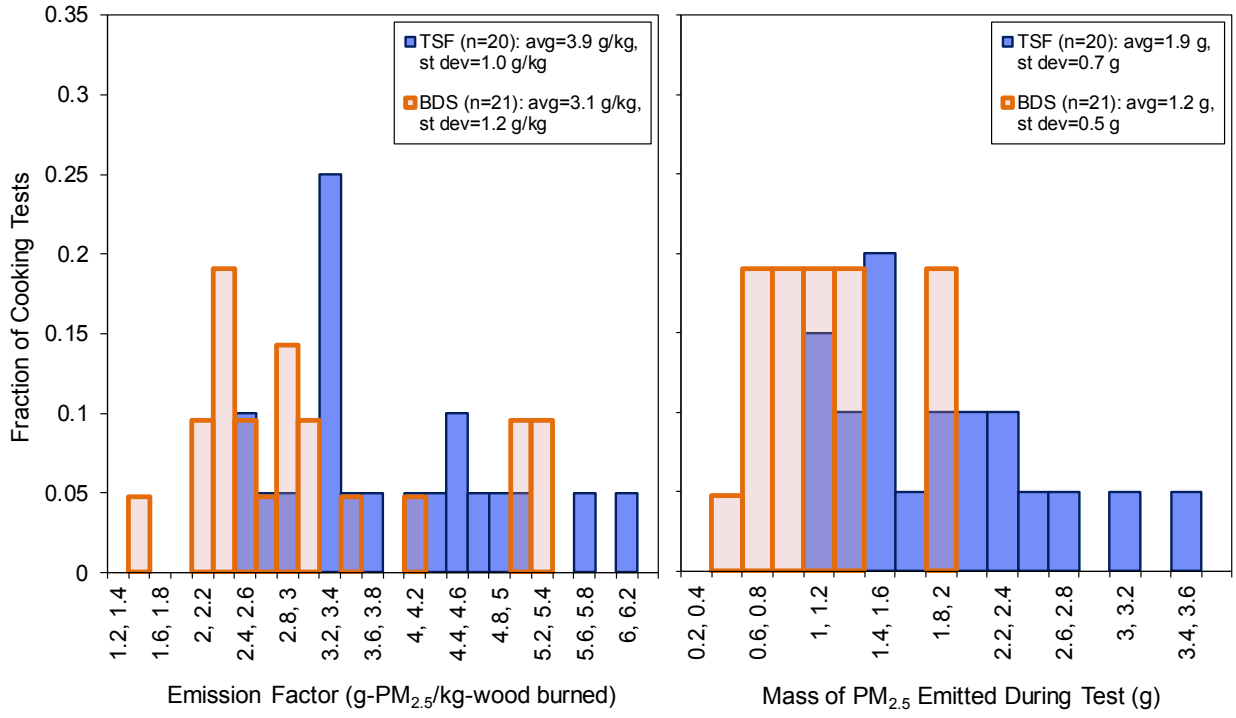

Figure 12: Distribution of BC fuel-based emission factor (left) and mass of BC emitted (right) in cooking tests with the BDS and TSF

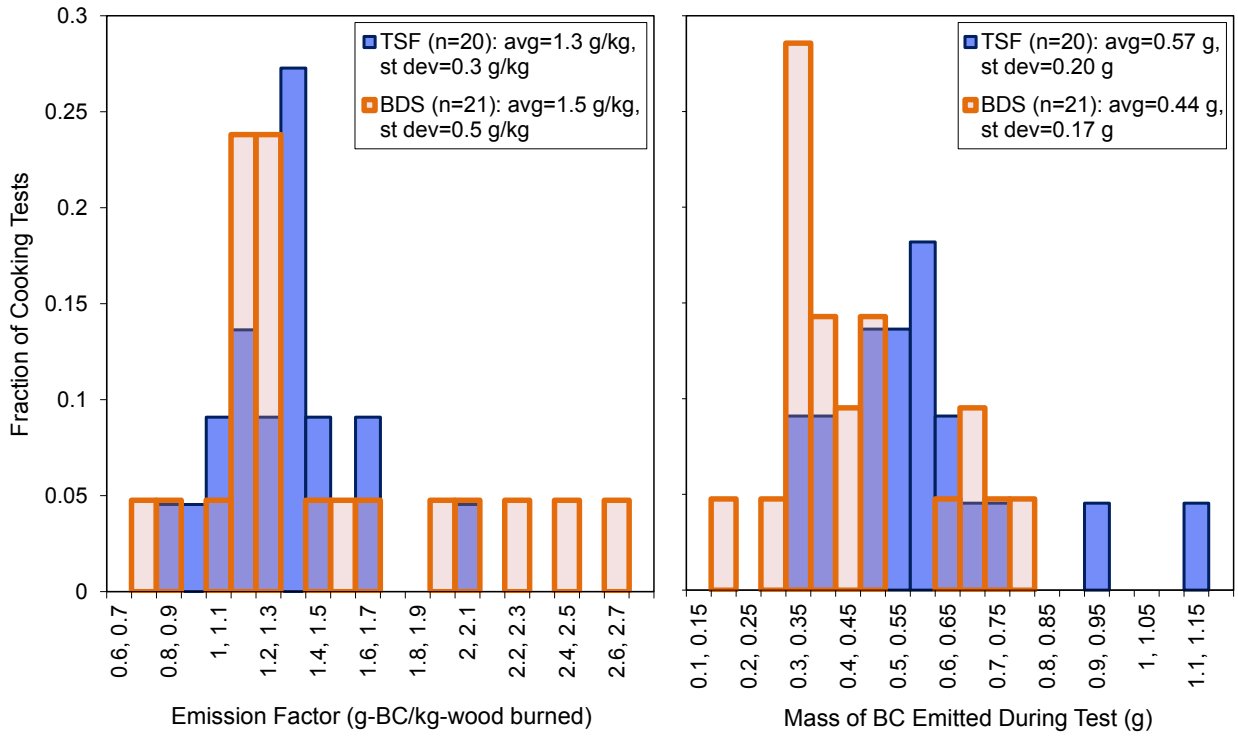

Figure 13: Distribution of BC/$PM_{2.5}$ emission ratio in cooking tests with the BDS and TSF

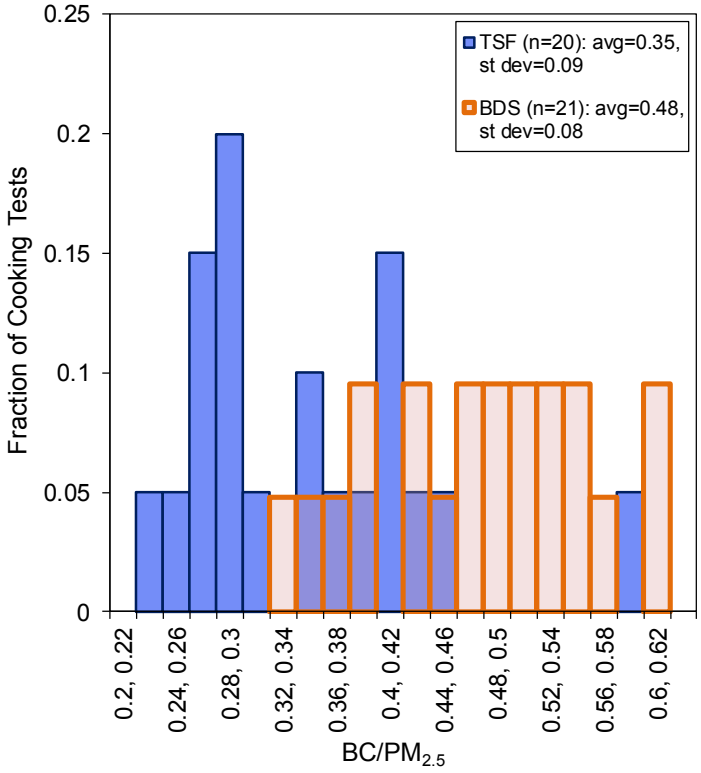

Figure 14: Distribution of $PM_{2.5}$ mass absorption efficiency (left) and mass scattering efficiency (right) in tests with the BDS and TSF

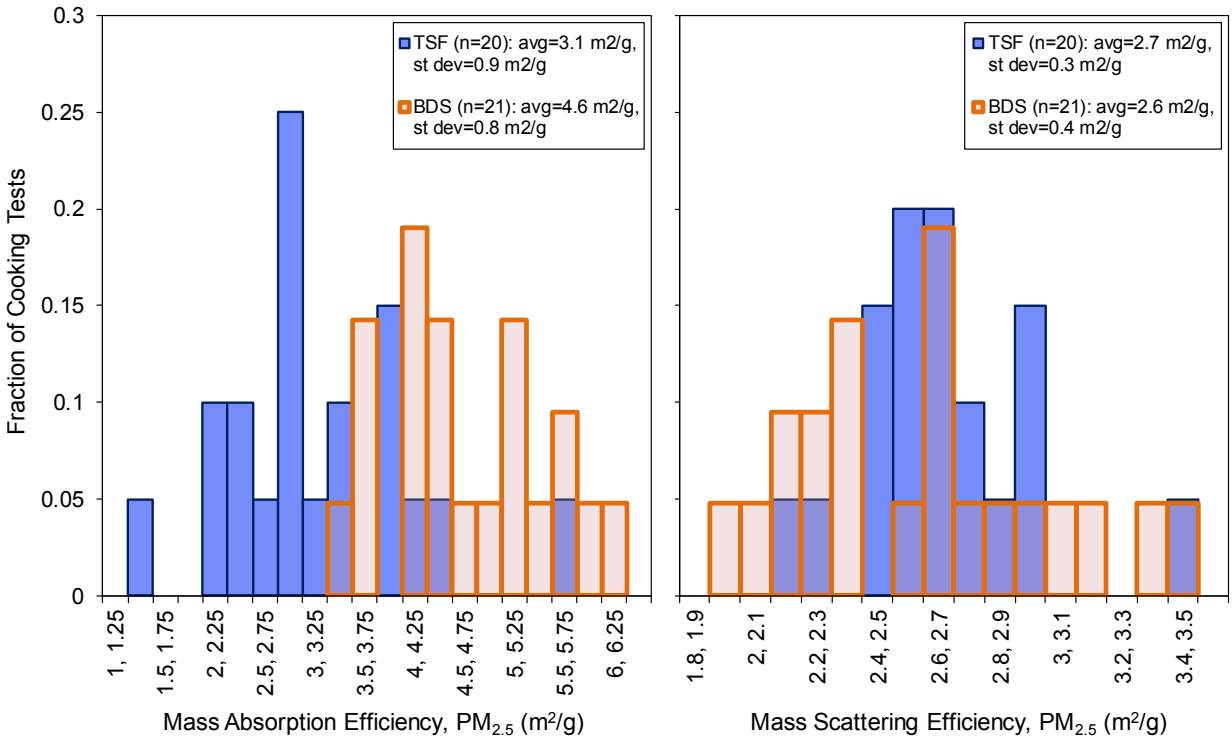

Figure 15: Distribution of $PM_{2.5}$ extinction-weighted single scattering albedo (left) and absorption Angstrom exponent (right) in tests with the BDS and TSF

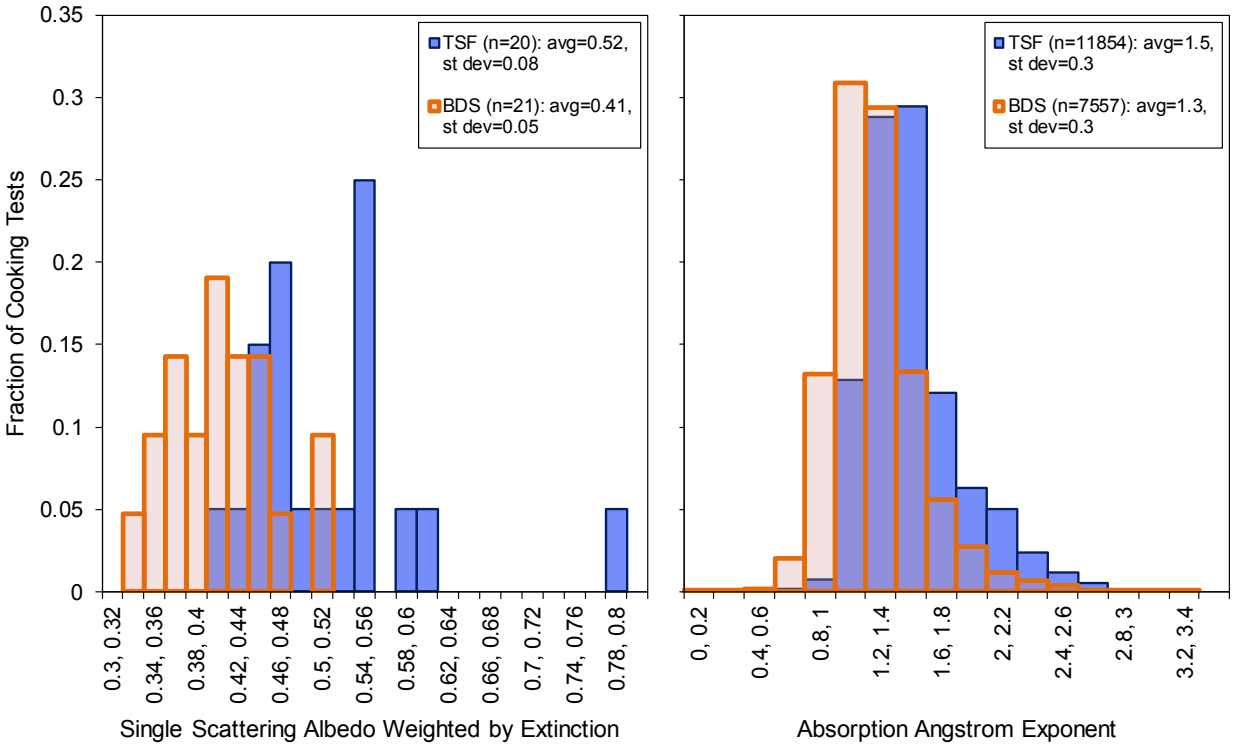

The average BC emission factor (g kg^{-1}) during tests with the BDS was 115% of that for the TSF. In terms of mass emitted, on average the BDS emitted 77% of the BC emitted during tests with the TSF. BC emissions showed a large degree of test-to-test variability and the distribution of BC emissions with BDS and TSF overlapped considerably.

Since the BDS reduced $PM_{2.5}$ emissions more than BC emissions, relative to the TSF, the emission ratio of BC/$PM_{2.5}$ was larger for the BDS. (Figure 13). This compositional difference is reflected in the higher $PM_{2.5}$ MAE_{532nm} (Figure 14, BDS/TSF = 148%), lower SSA (Figure 15), and lower AAE (Figure 15) in BDS smoke compared to TSF smoke. The lower SSA (0.41 for BDS, 0.52 for TSF) means that BDS smoke absorbs a greater fraction of incident light than TSF smoke: 59% versus 48%, respectively, based on the SSA complement (i.e., 1 – SSA). The lower AAE (1.26 for BDS, 1.51 for TSF) means that on the whole the BDS smoke is blacker than the TSF smoke. (Note that Figure 15 reports 1 Hz rather than test-average values of AAE.)

3.2 Instantaneous Emissions

The cumulative emission of CO, $PM_{2.5}$, and BC, based on instantaneous emission factors calculated with equation 10, is shown for five BDS (Figure 16) and five TSF (Figure 17) tests. In these figures, the mass emission of each pollutant is normalized to the total mass emitted in each test, such that as the test proceeds, the cumulative emission curves rise on the

Figure 16: Normalized cumulative emission of pollutants (y-axis) during BDS tests (x-axis shows the minutes since the start of each test)

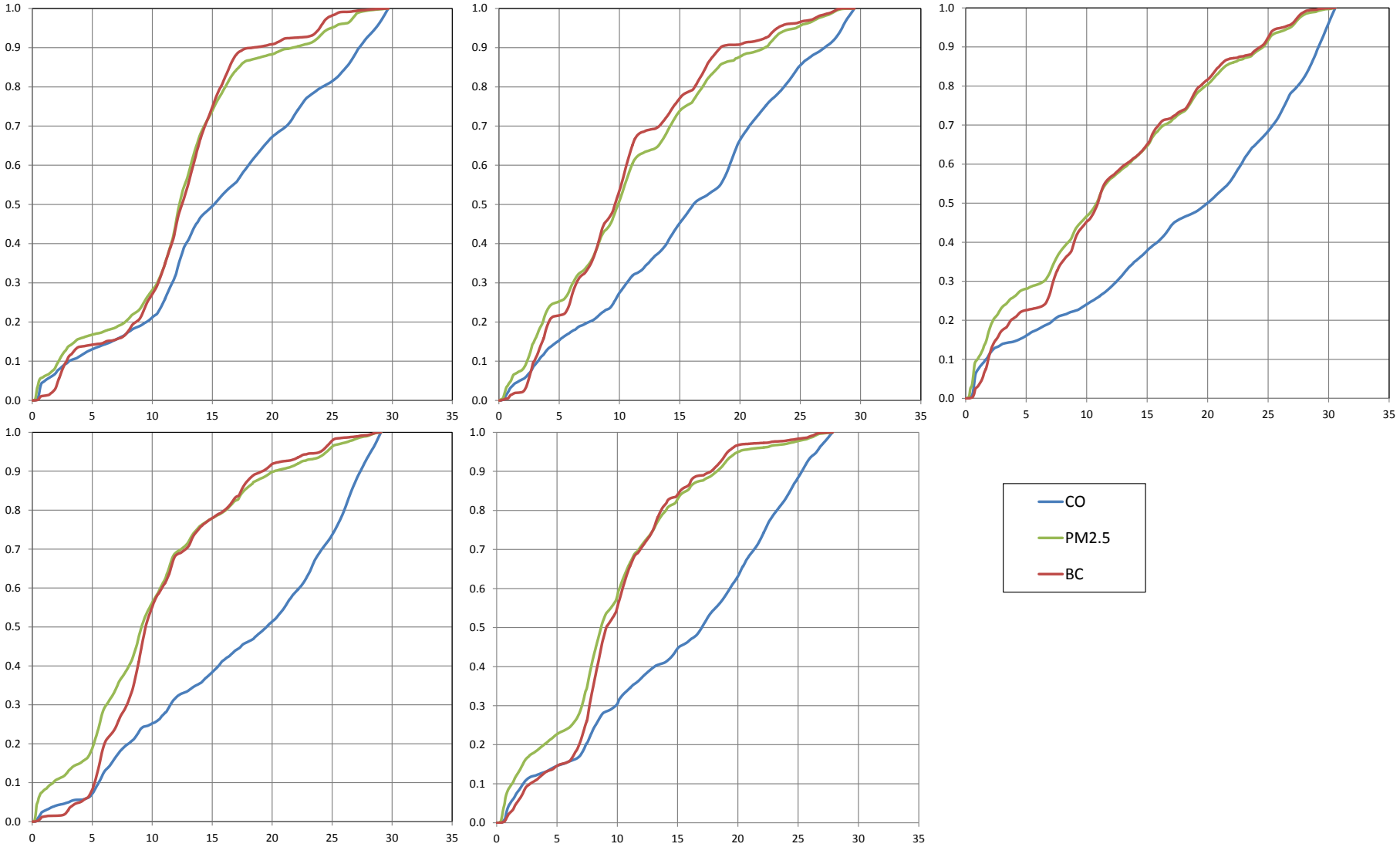

Figure 17: Normalized cumulative emission of pollutants (y-axis) during TSF tests (x-axis shows the minutes since the start of each test)

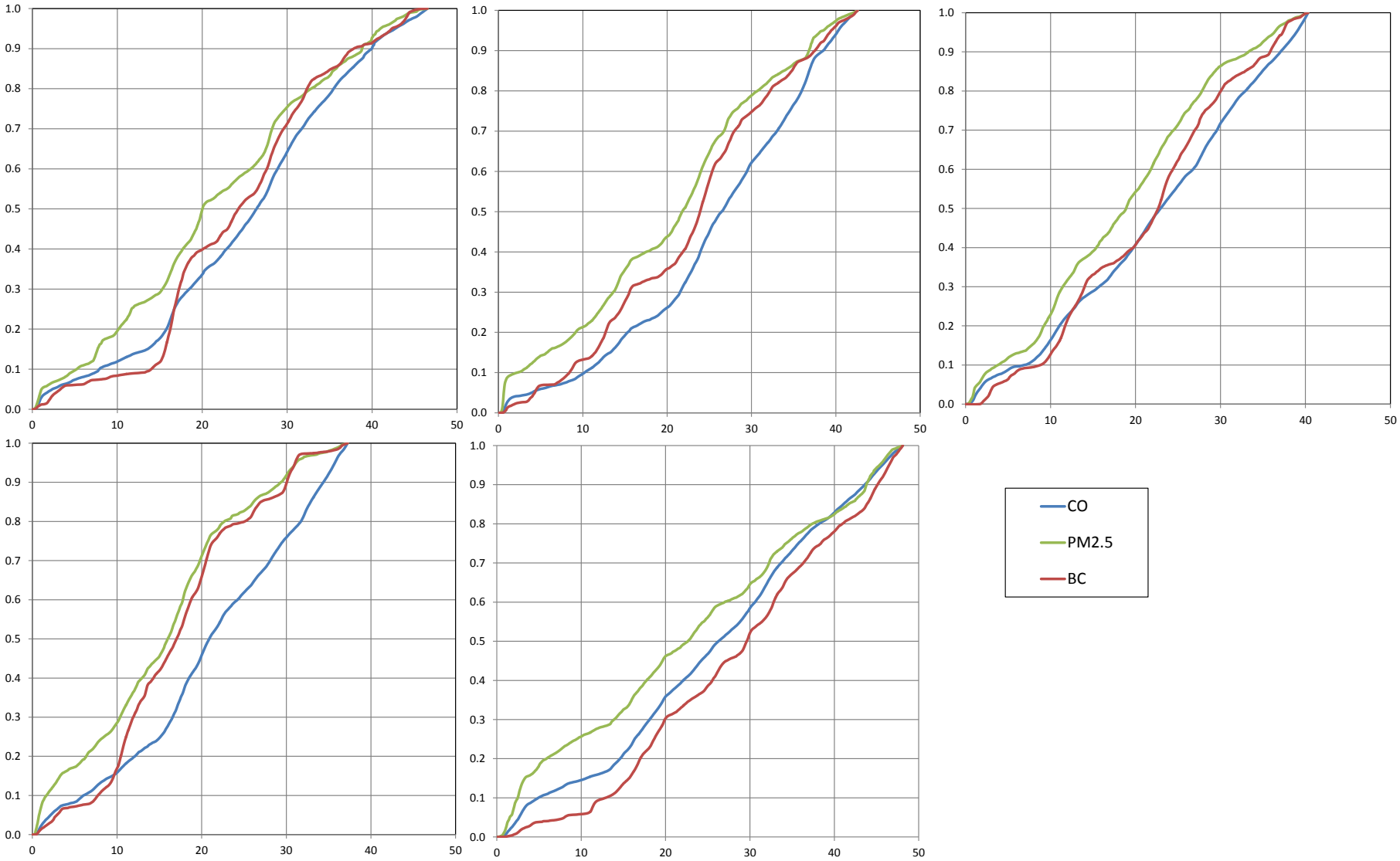

vertical axis from 0 to 1 (i.e., from 0 to 100% of the pollutant mass emitted during the test). The slope of the curves at every point indicates the mass emission rates of the pollutants.

A notable difference in the temporal pattern of emissions is evident when comparing the BDS and TSF test results. In general, $PM_{2.5}$ and BC emission rates were highest during the first half of BDS tests, which corresponded to the pre-boiling portion of these tests. As a result, most (65-80%) of the $PM_{2.5}$ and BC was emitted in the first half of BDS tests. The opposite was generally true of the CO emission rate during BDS tests, though the distinction between the first and second half (pre- and post-boiling portions) of BDS tests was less pronounced for CO than it was for $PM_{2.5}$ and BC. As a result, a minority (35-50%) of the CO was emitted in the first half of BDS tests. The higher emission rate of BC and the lower emission rate of CO during the pre-boiling portion of BDS tests suggest that the fire during this "high power" phase was more flaming and more combustion-efficient than during the subsequent "low power" phase.

By contrast, the emission rates of $PM_{2.5}$ and BC were more uniform throughout TSF tests than they were throughout BDS tests. About half (45-65%) of the $PM_{2.5}$ and half (35-60%) of the BC was emitted in the first half of TSF tests. The difference in pollutant emission rates between the pre- and post-boiling portions of BDS tests and the lack of such distinction in TSF tests is evidence that the combustion processes of these two stoves are different.

CHAPTER 4: Implications

The main design features of the BDS – most notably the containment of the flame in the frame upon which the pot sits – ensure that more of the heat of combustion reaches the pot than it does when cooking with the TSF. The thermal efficiency features of the BDS are present in improved stoves intended for application in other developing regions around the world (Still and Kness, 2010). The current study shows that, in addition to the improved thermal efficiency that leads to increased fuel efficiency, the combustion efficiency of the BDS is higher than that of the TSF. In this study of the BDS, the combined effects of increased fuel and combustion efficiencies reduced CO and $PM_{2.5}$ emissions each by forty percent, without significantly changing BC emissions when compared to the TSF.

Other similarly designed fuel-efficient stoves may share the co-benefit of reduced pollutant emissions. The study of Smith-Sivertsen et al. (2009), for example, showed that improved cookstoves in Guatemala reduced indoor air pollution and the occurrence of chronic respiratory symptoms. Wide implementation of improved stoves could abate the harmful effects of smoke exposure from traditional cookstoves in many developing regions.

The potential to reduce CO_2 emissions by replacing traditional cookstoves with improved cookstoves has prompted the consideration of using improved stoves as a global-warming abatement mechanism (e.g., Johnson et al., 2009). The present study confirms the CO_2 reduction potential of improved stoves: the BDS consumed 65% of the mass of wood consumed by the TSF. This study also found that the particles emitted from the BDS (SSA=0.41) were more light-absorbing than those emitted from the TSF (SSA=0.52). Based on the measured SSA values, particulate matter emitted by the BDS absorbs 20% more light (at 532 nm) than particulate matter emitted by the TSF ([1-0.41]/[1-0.52]=1.2). Also, the BDS emitted roughly sixty percent of the mass of particulate matter emitted by the TSF. Therefore, replacing traditional stoves with improved stoves may impact climate via changes to both particulate matter and CO_2 emissions.

A number of studies have demonstrated that the efficiency and emissions of cookstoves are highly variable and that stove performance in the field may be quite different than it is in the laboratory (MacCarty et al., 2008; Roden et al. 2009). Therefore, the results of the current study may not reflect the relative performance of the BDS and TSF in Darfur and may not be representative of the field performance of improved stoves similar to the BDS. Future research on cookstoves should continue to compare laboratory and field performance and aim to identify and understand factors that introduce variability, so that the benefits of improved stoves can be quantified with certainty.

CHAPTER 5: References

Abdollah, T (2008, March 28) Soot may play big role in climate, *Los Angeles Times*, retrieved from http://articles.latimes.com/2008/mar/25/nation/na-carbon25/2.

Andreae, MO; Gelenscér, A (2006) Black carbon or brown carbon? The nature of light-absorbing carbonaceous aerosols, *Atmos. Chem. Phys., 6,* 3131–3148.

Arnott, WP; Moosmüller, H; Rogers, CF; Jin, T; Bruch, R (1999) Photoacoustic spectrometer for measuring light absorption by aerosol: instrument description, *Atmos. Environ., 33,* 2845-2852.

Arnott, WP; Moosmüller, H; Walker, JW (2000) Nitrogen dioxide and kerosene-flame soot calibration of photoacoustic instruments for measurement of light absorption by aerosols, *Rev. Sci. Instrum., 71,* 4545-4552.

Barnett, TP; Adam, JC; Lettenmaier, DP (2005) Potential impacts of a warming climate on water availability in snow-dominated regions, *Nature, 438,* 303-309.

Bond, TC; Anderson, TL; Campbell, D (1999) Calibration and intercomparison of filter-based measurements of visible light absorption by aerosols, *Aerosol Sci. Tech, 30,* 582-600.

Bond, TC; Streets, DG; Yarber, KF; Nelson, SM; Woo, JH; Klimont, Z (2004) A technology-based global inventory of black and organic carbon emissions from combustion, *J. Geophys. Res., 109,* D14203, doi: 10/1029/2003JD003697.

Cappa, C; Lack, D; Burkholder, J; Ravishankara, AR (2008) Bias in filter-based aerosol light absorption measurements due to organic aerosol loading: evidence from laboratory measurements, *Aerosol Sci. Tech., 42,* 1022-1032.

Flanner, MG; Zender, CS; Randerson, JT; Rasch, P (2007) Present-day climate forcing and response from black carbon in snow, *J. Geophys. Res., 112,* D11202, doi:10.1029/2006JD008003.

Galitsky, C; Gadgil, A; Jacobs, M; Lee Y (2006) Fuel efficient stoves for Darfur camps of internally displaced persons report of field trip to North and South Darfur, Nov. 16-Dec.17, 2005, Lawrence Berkeley National Laboratory, LBNL-59540.

Gaur, S; Reed (1998), TB *Thermal Data for Natural and Synthetic Fuels*; Marcel Dekker: New York.

Hadley, OL; Ramanathan, V; Carmichael, GR; Tang, Y; Corrigan, CE; Roberts, GC; Mauger, GS (2007) Trans-Pacific transport of black carbon and fine aerosols (D < 2.5 μm) into North America, *J. Geophys. Res., 112,* D05309, doi:10.1029/2006JD007632.

Hadley, OL; Corrigan, CE; Kirchstetter, TW; Cliff, SS; Ramanathan, V (2010) Measured black carbon deposition on the Sierra Nevada snow pack and implication for snow pack retreat, *Atmos. Chem. Phys., 10,* 7505-7513.

Hadley, OL; Corrigan, CE; Kirchstetter, TW (2008) Modified thermal-optical analysis using spectral absorption selectivity to distinguish black carbon from pyrolized organic carbon, *Environ. Sci. Technol., 42,* 8459–8464.

Hansen, J; Nazarenko, L (2003) Soot climate forcing via snow and ice albedos, *Proc. Natl. Acad. Sci., 101*, 423-428.

Huang, L; Gong, SL; Sharma, S; Lavoué, D; Jia, CQ (2010) A trajectory analysis of atmospheric transport of black carbon aerosols to Canadian high Arctic in winter and spring (1990–2005), *Atmos. Chem. Phys., 10,* 5065-5073.

Johnson, M; Edwards, R; Ghilardi, A; Berrueta, V; Gillen, D; Frenk, CA; Masera, O (2009) Quantification of carbon savings from improved biomass cookstove projects, *Environ. Sci. Technol., 43,* 2456-2462.

Kirchstetter, TW; Novakov, T (2007) Controlled generation of black carbon particles from a diffusion flame and applications in evaluating black carbon measurement methods. *Atmos. Environ., 41*, 1874-1888, doi:10.1016/j.atmosenv.2006.10.067.

Kirchstetter, TW; Novakov, T; Hobbs, PV (2004) Evidence that the spectral dependence of light absorption by aerosols is affected by organic carbon, *J. Geophys. Res., 109,* D21208, doi:10.1029/2004JD004999.

MacCarty, N; Still, D; Ogle, D; Drouin, T (2008) Assessing cook stove performance: field and lab studies of three rocket stoves comparing the open fire and traditional stoves in Tamil Nadu, India on measures of time to cook, fuel use, total emissions, and indoor air pollution, retrieved from http://www.aprovecho.org/web-content/publications/assets/India%20CCT%20Paper_1.7.08.pdf

Menon, S; Hansen, J; Nazarenko, L; Luo, YF (2002) Climate effects of black carbon aerosols in China and India. *Science*, 297, 2250-2253.

NOAA, National Oceanic and Atmospheric Administration (2010) CalWater, retrieved from http://www.esrl.noaa.gov/psd/calwater/.

Penaloza, MA (1999) Deriving the basic cell-reciprocal integrating nephelometer equation and its use for calibration purposes: a comprehensive approach, *Meas. Sci. Technol., 10,* R1-R15.

Qian, Y; Gustafson, WI; Leung, LR; Ghan, SJ (2009) Effects of soot-induced snow albedo change on snowpack and hydrological cycle in western United States based on weather research and forecasting chemistry and regional climate simulations, *J. Geophys. Res., 114,* D03108, doi:10.1029/2008JD011039.

Ramanathan, V; Carmichael, G (2008) Global and regional climate changes due to black carbon, *Nat. Geosci., 1,* 221-227.

Roden, CA; Bond, TC; Conway, S; Pinel, ABO; MacCarty, N; Still, D (2009) Laboratory and field investigations of particulate and carbon monoxide emissions from traditional and improved cookstoves, *Atmos. Environ., 43,* 1170-1181.

Rosenfeld, D; Givati, A (2006) Evidence of orographic precipitation suppression by air pollution–induced aerosols in the western United States. *J. Appl. Meteorol. Clim., 45,* 893–911.

Rosenthal, E (2009, April 16) Third-world stove soot is target in climate fight, *New York Times,* retrieved from http://www.nytimes.com/2009/04/16/science/earth/16degrees.html?_r=1.

Smith-Sivertsen, T; Diaz, E; Pope, D; Lie, RT; Diaz, A; McCracken, J; Bakke, P; Arana, B; Smith, KR; Bruce, N (2009) Effect of reducing indoor air pollution on women's respiratory symptoms and lung function: the RESPIRE randomized trial, Guatemala, *Am. J. Epidemiol., 170*, 211-220.

Stewart, IT; Cayan, DR; Dettinger, MD (2004) Changes in snowmelt runoff timing in western North America under a "business as usual" climate change scenario, *Climatic Change, 62,* 217-232.

Still, D; Kness, J (2010) Capturing heat: five earth-friendly cooking technologies and how to build them, Aprovecho Research Center document, retrieved from http://weblife.org/capturing_heat/pdf/capturing_heat.pdf.

USDOS, U.S. Department of State (September 2010) Global alliance for clean cookstoves: the United States commitment by the numbers, retrieved from http://www.state.gov/r/pa/prs/ps/2010/09/147494.htm.

Virkkula, A; Ahlquist, NC; Covert, DS; Arnott, WP, Sheridan, PJ; Quinn, PK; Coffman, DJ (2005) Modification, calibration and field test of an instrument for measuring light absorption by particles, *Aerosol Sci. Technol*., *39*, 68-83.

WHO, World Health Organization (June 2005) Fact sheet no. 292: indoor air pollution and health, retrieved from http://www.who.int/mediacentre/factsheets/fs292/en/index.html.

Wallmo, K; Jacobson, SK (1998) A social and environmental evaluation of fuel-efficient cook-stoves and conservation in Uganda, *Environ. Conserv.,25,* 99-108.

CHAPTER 6: Glossary

ATN	attenuation: a measure of amount of light absorbed by particles collected on the filter inside the aethalometer
AAE	absorption □ngstrom exponent: a measure of the variation of particulate matter light absorption with wavelength
b_{abs}	particulate matter light absorption coefficient (Mm^{-1})
b_{scat}	particulate matter aerosol light scattering coefficient (Mm^{-1})
BC	black carbon: the black portion of carbonaceous soot
BDS	Berkeley-Darfur Stove
CO	carbon monoxide
CO_2	carbon dioxide
ext	extinction: the sum of absorption and scattering
MAE	mass absorption efficiency: a measure of how much light is absorbed by particulate matter
MSE	mass scattering efficiency: a measure of how much light is scattered by particulate matter
RH	relative humidity: a measure of the amount of water vapor present in the air
PAS	photoacoustic absorption spectrometer: an instrument that measures the absorption coefficient of particulate matter and, in this study, an instrument that was also equipped with a reciprocal nephelometer
$PM_{2.5}$	particle matter less than 2.5 micrometers in diameter
PSAP	particle soot absorption photometer: a filter-based instrument that operates much like the aethalometer but measures aerosol absorption coefficient instead of black carbon concentration
σ	sigma: a calibration constant used by the Aethalometer to convert particle light absorption to BC mass concentration
SSA	single scattering albedo: the fraction of incident sunlight that is scattered instead of absorbed, a parameter that determines whether an aerosol is climate-warming or climate-cooling
TOA	thermal-optical analysis: a method of measuring the amount of carbon in particulate matter

TSF	three-stone fire: an arrangement of three stones that support a pot over an open fire is the traditional cooking “stove” in many developing regions of the world

APPENDIX A: Pollutant Concentrations and Emissions

Table A1: Test duration, mass and moisture content of wood combusted, and average pollutant concentrations and optical properties measured during BDS tests

Test	Duration (min)	Dry Wood Combusted (g)	Wood Moisture (%)	ΔCO_2 (ppm)	CO (ppm)	$PM_{2.5}$ (mg m^{-3})	BC (mg m^{-3})	Abs (Mm^{-1})	Scat (Mm^{-1})
01	31.4	351	7.1	477	74	5.1	3.1	29165	14142
02	31.2	322	7.4	484	60	4.1	2.4	25013	10790
03	29.9	438	11.2	464	97	7.0	3.1	24096	18344
04	32.6	390	10.2	520	61	5.8	2.3	20517	11466
05	34.2	429	10.3	491	73	5.9	2.5	24552	13741
06	33.3	421	10.7	482	84	6.4	3.3	26082	16750
07	29.7	375	8.6	534	69	6.5	3.5	36534	20105
08	29.5	338	7.2	542	58	4.8	2.4	28780	12435
09	33.4	413	9.9	473	73	6.0	2.3	25311	13531
10	30.5	375	9.2	518	89	6.9	2.5	25509	15003
11	29.1	326	9.1	534	71	4.5	1.4	19624	9472
12	27.9	337	8.9	549	76	4.4	2.6	22658	11424
13	30.6	352	9.2	584	67	3.0	1.6	15397	6337
14	28.4	359	9.4	536	78	4.9	2.6	23251	11375
15	30.3	352	9.5	580	71	4.1	2.1	17916	9779
16	28.3	353	10.5	597	72	5.0	2.3	21332	11275
17	26.9	333	8.0	593	117	9.8	4.6	43280	28240
18	30.0	363	8.1	551	81	11.8	5.7	62651	40342
19	33.2	378	7.8	573	77	10.9	4.7	51635	31790
20	28.3	373	8.0	575	112	12.8	5.0	44936	39400
21	27.4	351	7.8	628	101	12.4	6.2	62961	42111

Table A2: Test duration, mass and moisture content of wood combusted, and average pollutant concentrations and optical properties measured during TSF tests

Test	Duration (min)	Dry Wood Combusted (g)	Wood Moisture (%)	ΔCO_2 (ppm)	CO (ppm)	$PM_{2.5}$ (mg m^{-3})	BC (mg m^{-3})	Abs (Mm^{-1})	Scat (Mm^{-1})
01	40.0	540	7.0	455	105	8.0	3.5	31141	23811
02	42.1	505	7.2	480	107	6.1	2.8	23715	16418
03	48.1	624	11.3	471	132	12.0	2.8	16704	41539
04	48.2	655	9.5	484	92	9.3	2.5	20162	24894
05	45.7	633	9.6	500	108	9.5	2.8	22159	23364
06	46.5	522	9.7	529	79	7.6	2.1	18170	21065
07	34.7	496	7.0	544	114	7.7	3.2	30877	20156
08	50.4	737	10.8	471	97	9.2	2.4	25395	24264
09	35.2	558	9.0	511	116	11.3	3.0	25180	28612
10	33.3	458	9.1	558	112	7.4	1.9	19418	15541
11	42.6	538	9.3	476	89	6.3	2.2	17873	15850
12	34.8	482	9.3	572	108	5.5	2.2	18135	13425
13	42.4	511	9.0	546	96	5.3	2.1	16226	11822
14	40.3	568	9.9	536	100	6.6	2.7	21864	17204
15	37.3	500	10.8	568	97	5.0	1.9	18844	12062
16	35.5	538	10.9	553	139	8.2	2.8	22771	20921
17	34.6	494	7.8	589	102	9.9	3.0	43155	27338
18	50.3	671	7.9	496	104	13.2	3.8	36571	39460
19	39.0	640	7.6	551	99	9.8	5.7	54320	28298
20	39.8	615	7.9	581	121	12.2	3.6	33866	35675

Table A3: Emissions and optical properties of pollutants during BDS tests

Test	Emission Factor (g kg^{-1})			Total Mass Emitted (g)			MAE (m^2 g^{-1})	MSE (m^2 g^{-1})	SSA *
	CO	$PM_{2.5}$	BC	CO	$PM_{2.5}$	BC			
01	40	2.5	1.5	15	0.8	0.44	5.7	2.8	0.40
02	35	2.1	1.2	12	0.7	0.33	6.0	2.6	0.35
03	46	2.9	1.3	20	1.4	0.48	3.4	2.6	0.51
04	36	3.0	1.2	16	1.3	0.36	3.5	2.0	0.44
05	40	2.8	1.2	17	0.8	0.45	4.2	2.3	0.38
06	44	2.9	1.5	20	1.3	0.61	4.1	2.6	0.51
07	38	3.1	1.7	15	1.1	0.49	5.6	3.1	0.40
08	33	2.4	1.2	14	0.8	0.33	6.0	2.6	0.34
09	39	2.8	1.1	18	1.2	0.33	4.2	2.2	0.37
10	50	3.4	1.2	20	1.3	0.36	3.7	2.2	0.43
11	41	2.3	0.7	16	1.1	0.20	4.4	2.1	0.40
12	42	2.1	1.3	16	0.7	0.34	5.2	2.6	0.40
13	39	1.5	0.8	17	0.5	0.26	5.1	2.1	0.33
14	41	2.2	1.2	16	1.3	0.36	4.8	2.3	0.38
15	44	2.2	1.2	21	0.8	0.31	4.4	2.4	0.41
16	40	2.5	1.1	19	0.8	0.32	4.2	2.2	0.42
17	56	4.1	1.9	18	0.5	0.45	4.4	2.9	0.42
18	41	5.2	2.5	15	1.6	0.77	5.3	3.4	0.44
19	42	5.2	2.3	17	1.8	0.69	4.7	2.9	0.45
20	53	5.3	2.1	21	2.3	0.70	3.5	3.1	0.48
21	50	5.4	2.7	17	1.5	0.74	5.1	3.4	0.45

* single scattering albedo weighted by total extinction

Table A4: Emissions and optical properties of pollutants during TSF tests

Test	Emission Factor (g kg^{-1})			Total Mass Emitted (g)			MAE (m^2 g^{-1})	MSE (m^2 g^{-1})	SSA*
	CO	$PM_{2.5}$	BC	CO	$PM_{2.5}$	BC			
01	56	3.7	1.6	27	2.1	0.65	3.9	3.0	0.50
02	59	3.0	1.4	30	1.4	0.57	3.9	2.7	0.48
03	76	6.0	1.4	39	3.5	0.67	1.4	3.5	0.78
04	52	4.6	1.2	29	3.8	0.57	2.2	2.7	0.55
05	59	4.5	1.3	30	2.4	0.56	2.3	2.5	0.53
06	55	4.6	1.3	24	2.5	0.45	2.4	2.8	0.61
07	56	3.3	1.3	28	1.6	0.51	4.0	2.6	0.43
08	51	4.2	1.1	32	3.2	0.58	2.8	2.6	0.55
09	60	5.1	1.4	26	2.6	0.47	2.2	2.5	0.59
10	58	3.3	0.8	25	1.5	0.31	2.6	2.1	0.47
11	52	3.2	1.1	23	1.6	0.46	2.8	2.5	0.55
12	58	2.6	1.0	26	1.1	0.39	3.3	2.4	0.45
13	57	2.7	1.1	25	1.5	0.38	3.1	2.2	0.46
14	56	3.2	1.3	26	1.5	0.61	3.3	2.6	0.48
15	55	2.5	0.9	26	1.1	0.33	3.8	2.4	0.47
16	65	3.3	1.2	34	1.7	0.50	2.8	2.6	0.46
17	49	4.1	1.2	23	2.0	0.52	4.4	2.8	0.46
18	52	5.8	1.7	39	5.6	0.93	2.8	3.0	0.54
19	41	3.5	2.1	25	2.2	1.14	5.5	2.9	0.41
20	55	4.8	1.4	32	3.0	0.75	2.8	2.9	0.54

* single scattering albedo weighted by total extinction